JOURNAL OF THERMOPHYSICS AND HEAT TRANSFER
Vol. 7, No. 1, Jan.–March 1993

Survey of Measurements of Flow Properties in Arcjets

Carl D. Scott
NASA Johnson Space Center, Houston, Texas 77058

Nomenclature

A_{ij} = transition probability
A^* = nozzle throat area
C_P = pressure coefficient
C_p = specific heat
c = speed-of-light
E = energy
f = oscillator strength
g = statistical weight
h = Planck constant
h_N = enthalpy of formation of nitrogen atoms
h_T, h_t = total specific enthalpy
h_0 = centerline enthalpy
I = intensity
I = current
J = current
K^I, K^{II} = rotational quantum numbers of upper and lower states, respectively
k = Boltzmann constant
m = mass
m_g = gas flow rate
N = number of molecules
n = number density
n_e = electron density
P_{T1} = total pressure
p_s = stagnation point pressure
Q = partition function
q_s = stagnation point heat flux
R_{cyl} = radius of cylinder
R_{eff} = effective radius of body (equivalent sphere)
r = radial distance
r_e = electron radius
T = temperature
t = time
u = velocity
V = velocity
X = distance from leading edge
Y = distance from surface
Z = axial distance
ε = emission
λ = wavelength
ν_{ij} = frequency of transition from state i to j
ρ = density

Subscripts
calc = calculated
cw = cold wall
e = electron
i = state "i"
m = metastables
w = evaluated at wall
0 = ground state
∞ = freestream

Introduction

TESTING of the spacecraft thermal protection materials and systems to determine their performance is usually done in an arc-heated wind tunnel or test facility. Samples of the material are immersed in the high enthalpy flow and heated to a temperature or level of heat flux to simulate the local flight environment. Test articles, constructed to represent local spacecraft structures, are subjected to heating profiles that test the capability of the materials and structures to withstand the anticipated local flight environment. How well the test simulates conditions is determined by predicting the local flight environment and comparing the predictions with the measurements of the arcjet flow environment. Determining the arcjet environment requires complex analytical and experimental procedures. The accuracy of the simulation often depends on the ability to measure the flow properties and to control these properties within the capability of the facility.

Arcjet facilities are also used to determine the rates of energy accommodation in catalytic recombination of atoms on surfaces. This requires detailed knowledge of the flow conditions (including freestream and shock layer flow composition), velocity, and density, in order to calculate the heating that results from both thermal convection as well as species diffusion.

This paper addresses methods for determining enthalpy, pressure, temperature, velocity, and species-excited state populations of the flow. Because arcjet flows are usually in thermal and chemical nonequilibrium, determinations of the

Carl D. Scott received his B.A. degree in physics from Rice University and his Ph.D. in physics from the University of Texas at Austin. He joined NASA's Johnson Space Center after service in the Navy. In his early years at JSC, he studied arcjet plasma and flow diagnostics and did his Ph.D. dissertation on spectral line broadening of helium in arcjet flows. As a research engineer and Aerothermodynamics Group Leader in the Aeroscience Branch, he has done experimental and theoretical work in the aerothermodynamic areas of catalytic atom recombination, reacting flowfields, and associated convective heating for the Space Shuttle Orbiter, aeroassisted space transfer vehicles, and the Aeroassist Flight Experiment. He recently spent a year at the Université Paris Nord (France) as a visiting professor developing a chemical and thermal nonequilibrium model of a hydrogen plasma applicable to diamond deposition plasmas. Dr. Scott is an Associate Fellow of the AIAA, a past member of the Thermophysics Technical Committee, and has been technical program chairman and general chairman of AIAA conferences.

Presented as Paper 90-1765 at the AIAA Thermophysics Conference, June 18–20, 1990, Seattle, WA; received July 31, 1990; revision received Jan. 13, 1992; accepted for publication Feb. 6, 1992.

various energy modes are needed; thus it is necessary to measure the vibrational, rotational, translational, electron, and excitation temperatures. Both intrusive and nonintrusive means for determining these flow properties are discussed herein. Table 1 shows the various flow properties to be discussed and the diagnostic techniques that may be used to determine them.

The use of arcjets that simulate re-entry into the Earth's atmosphere dates back to the 1950s; many of the techniques in use today to determine the flow characteristics date back to that time. In the 1960s, spectroscopic and electrostatic techniques were applied to diagnose the flow. However, these sophisticated techniques fell into disuse because of the major manpower commitment required, lack of funds, and the priority use of facilities to test materials and structures over understanding details of the flow. The main types of early diagnostics or characterization of the flows were heat flux, surface temperature, enthalpy, and pressure measurements. Even the enthalpy was relegated to a subordinate parameter as far as thermal testing of structures was concerned. However, when it became apparent that the Space Shuttle Orbiter thermal protection tiles and the leading-edge material were fairly noncatalytic with respect to atom recombination, there was increased interest in understanding the composition of the flow and its interaction with thermal protection materials. This has led to the implementation of modern spectroscopic and laser diagnostic techniques in arcjet facilities.

Although the development of diagnostic techniques for low-density nonequilibrium is rapidly advancing, this paper addresses only techniques that actually have been demonstrated as useful for measuring properties in arcjet flows—and mostly in arcjets used for materials testing.

Most of these techniques require a large amount of effort to carry out. They are not easy and are full of pitfalls. Therefore, to engage in a diagnostics program using these techniques requires a large commitment of personnel and facility time. These techniques may not be developed to the extent to which a definitive statement can be made about the range of conditions or accuracy may be assessed. Development effort is still needed in some cases to fully exploit the techniques.

Arcjet facilities have been applied to various flight regimes, from the high-pressure and high-heating environments of ballistic missile re-entry and planetary atmosphere entry to the relatively low-pressure environment associated with re-entries of lifting manned spacecraft. Most of this paper addresses the lower pressure regime because of the author's familiarity with it and because of the current interest in hypersonic manned flight. Although the atmosphere of primary interest is air, the arcjet flow of the atmosphere noble gases will be addressed briefly, because 1) these gases are simple and illustrate the diagnostic techniques; and 2) noble gases may be used as trace species for diagnostic purposes.

In the lower pressure regimes, the flow is not in chemical equilibrium and in many instances is not in thermal equilibrium. For example, the electrons may be at a different temperature from the heavy particles. Also, the vibrational state populations may deviate from a Boltzmann distribution. These nonequilibrium effects have a tendency to complicate the flow description and diagnostics. Therefore, to fully characterize the flow it is necessary to measure additional flow parameters. Measurements to determine these nonequilibrium phenomena and effects include spectroscopy, laser-induced fluorescence, direct mass spectrometry, and catalytic and electrostatic probes.

Measurement Parameters

Arc Heater Operational Parameters

Basic information about the operation of the arc heater itself is necessary for an understanding of the flow properties. In particular, the total pressure and enthalpy of the flow is derived from measurements of the arc heater operating conditions. (A discussion of the various methods used to determine the average total enthalpy of the flow is given by Pope.[1]) The bulk total enthalpy is obtained from the heat balance method. For the heat balance, the arc current, arc voltage, and mass flow rate of the gas are measured. Also, the heat lost to the walls of the heater is determined from the heat gain of the coolant. From these measurements the total enthalpy averaged over the flow is calculated using

$$h_T = \frac{IV - m_c C_p(\Delta T - \Delta T_0)}{m_g} \tag{1}$$

Table 1 Arcjet flow parameters and diagnostics techniques for their determination

Parameter	Measurement technique
Stagnation point pressure	Pitot probe with pressure transducer
Heat flux	Gardon gauge
	Slug calorimeter
Enthalpy	Energy balance
	Sonic throat technique
	Heat flux and stagnation pressure
Species concentrations	Mass spectrometer probe
Excitation temperature of atoms	Emission spectroscopy, line intensities
Rotational temperature of molecules	Emission spectroscopy
	Laser-induced fluorescence
	Electron beam fluorescence
Vibrational temperature of molecules	Intensity distribution
	Emission spectroscopy
	Absorption spectroscopy
	Laser-induced fluorescence
	Electron beam fluorescence
Static temperature of electrons	Emission spectroscopy,
	Continuum spectroscopy
	Doppler profiles, laser
	Thomson scattering
	Electrostatic probes
Static temperature of gas	Doppler profiles, laser-induced fluorescence
Velocity	Doppler laser-induced fluorescence
	Electrostatic probes
	Doppler laser Thomas scattering
Electron density	Electrostatic probes
	Emission spectroscopy
	Continuum intensity
	Stark line broadening

where the current is I, the voltage drop across the heater is V, m_c is the coolant flow rate, C_p is the specific heat of the coolant, ΔT is the temperature rise of the coolant, and ΔT_0 is the temperature increase of the coolant due to viscous effects in the coolant passages. Measurement of the temperature rise of the coolant with no arc yields ΔT_0. Because the temperature rise of the coolant is usually small it is necessary to take some precautions to measure it accurately. This is the major source of uncertainty in determining the bulk average enthalpy. To determine the enthalpy of the inviscid core of the jet only heat losses in the heater itself should be included in Eq. (1) and not the heat loss to a nozzle wall. To determine the mean enthalpy of the fully developed flow (as in a duct) the energy losses to the duct wall should be included. Also the nozzle losses should be included if the enthalpy integral (heat flux) method discussed below is to be used. Because Eq. (1) yields a bulk average, it does not reveal any information about the detailed enthalpy distribution in the flowfield.

Other techniques for determining the enthalpy of the flow are the sonic throat method (also called the sonic flow method) and the heat flux method. The sonic throat method will be addressed first. In its simplest form, the method depends on the assumption of perfect gas flow[1] or equilibrium flow.[2] However, if a nonequilibrium flow code is available, the method could be extended to nonequilibrium flow provided some reasonable starting conditions can be assumed—an assumption that is not always feasible. The total enthalpy of the flow is related to the stagnation pressure and the nozzle throat area by the relation

$$h_T \approx 0.0492 \left(\frac{P_{T1} A^*}{m_g} \right)^{2.5} \tag{2}$$

where the units are all in the international system of units (SI). The total pressure in an arc heater may be used to determine the enthalpy or total temperature if the flow can be considered in equilibrium upstream of the nozzle throat. Accurately determining the total pressure also needs careful attention. At the upstream end of the heater where the gas velocity of the flow is near zero, the stagnation pressure may be measured by a static pressure tap. However, this stagnation pressure is not the same as the stagnation pressure of the flow at the nozzle throat due to the heating and viscous effects in the arc heater.[3] Likewise, static pressure measurement at the nozzle throat is not an accurate measure of the stagnation pressure, since the flow is near sonic velocity. Relating the static pressure to stagnation pressure requires knowledge of the ratio of specific heats of the mixture and the Mach number. The Mach number at the nozzle throat is usually taken to be unity, but the location of the sonic line may not be accurately known due to the effect of the viscous boundary layer on the effective throat area. It should also be noted that there is often some slag or other contaminants in arc heaters which may foul or clog the orifice of the pressure tap and interfere with accurate measurements of the pressure. These considerations often make determining the enthalpy by the "sonic flow" method difficult.

Another difficulty with bulk methods such as the sonic flow and the energy balance enthalpy methods is that the flow in arc heaters is often not very uniform. Therefore, a local measure of the enthalpy is needed. One can make a determination of the local enthalpy using the heat flux method.[1,4] Because the heat flux to an object depends on the total enthalpy, a heat flux relation can be solved for the enthalpy. In the past, the Fay and Riddell[5] heating equation or a similar heat flux relation has been used to infer the enthalpy. In using this technique, the catalytic recombination efficiency of the surface of the heat flux sensor must be known or should be very large (effectively fully catalytic). The enthalpy can then be obtained from the measured heat flux and stagnation point pressure

$$h_T = C q_s \left(\frac{R_{\text{eff}}}{p_s} \right)^{1/2} \tag{3}$$

where C is a constant. The effective radius of the heat flux probe depends on the shape. Most probes are either spherical or flat-face cylinders. For spheres, the effective radius is simply the sphere radius. For flat-face cylinders, the effective radius must be determined analytically or by experiment. Hiester and Clark[4] found for the conditions of their series of tests in a number of arcjet facilities that

$$R_{\text{eff}} = R_{\text{cyl}}/0.54 \tag{4}$$

Actually, the factor, which depends on the velocity gradient, is a function of density ratio across the shock wave. Bade and Yos[6] in their nonequilibrium arcjet flow analysis, use a correlation of the measurements of Boison and Curtiss[7] for a flat-face cylinder.

Pope[1] compares the heat flux method with bulk flow methods by surveying the stream and integrating the enthalpy distribution across the stream using the relation

$$\frac{h_0}{\bar{h}} = \frac{m_g}{\pi \int_0^R \frac{h}{h_0} \rho u r \, dr} \tag{5}$$

where h_0 is the centerline enthalpy, $\bar{h}$ is the bulk average enthalpy, h is the local enthalpy, ρu is the local mass flux (assumed to be constant function of radius), and the integration is over the area of the flow cross section.

There has been much uncertainty in the enthalpy determined from two methods in various facilities as can be seen in Fig. 1 from Hiester and Clark[4] of the Stanford Research Institute (SRI). Figure 1 compares enthalpy determined from a slug calorimeter heat flux gauge with enthalpy determined from the sonic flow method. The units are Btu/lb in Fig. 1. Therefore, better techniques would be helpful. Nonintrusive techniques will give some of the parameters that make up the enthalpy in a nonequilibrium flow, such as the velocity and temperatures, but they are not likely to yield all modes of energy in the near future. Intrusive techniques such as electrostatic probes and mass spectroscopic probes yield additional information such as the electron temperature and species concentrations, respectively. However, these intrusive techniques may perturb the flow and have other uncertainties associated with them.

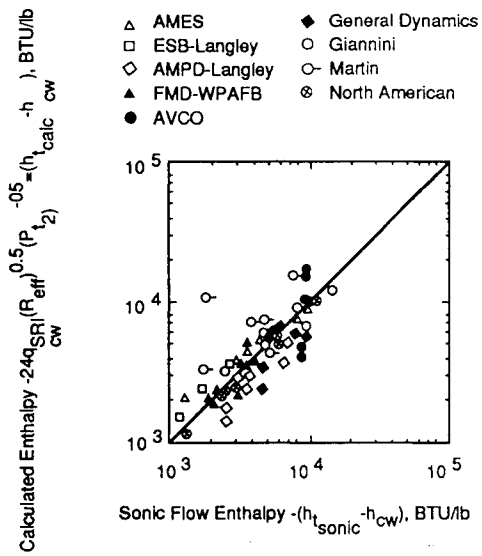

Fig. 1 Enthalpy calculated from heating rate vs sonic flow enthalpy.[4]

Flow Properties

The following sections will address various flow properties and diagnostic techniques that have been used in arcjet facilities.

Heat Flux Measurements

Heat flux probes have been discussed as a tool for determining the local total enthalpy. The heat flux is also used to set up test conditions for materials and structures testing. Usually the heat flux sensors are installed in models that have the same geometry as the test article. They are located in strategic positions where the incident heat flux is to be imposed on the test article—frequently the stagnation point.

Heat fluxes are commonly measured by two types of instruments in arcjet facilities where the heat flux ranges from about 1 W/cm^2 to more than 500 W/cm.^{2} For the most accurate work the slug calorimeter is often used because its output does not depend on a calibration. The response of the sensor is strictly a function of the geometry and physical properties of the slug, provided the slug is properly isolated from the supporting hardware. The heat flux is determined from the temperature rise rate of the slug of material, usually copper

$$q = mC_p \frac{dT}{dt} \tag{6}$$

An example of a slug type sensor is shown in Fig. 2 which is taken from Ref. 4. This type of sensor has been used successfully in many applications in which the surface coating could be varied to assess catalytic properties at low temperatures.[8] Also, slug calorimeters were used to measure the heat flux to nickel and Teflon® surfaces to assess slip and catalytic boundary equations[9] for a time-dependent relaxation computational fluid dynamics code.[10]

Another type of instrument for measuring heat flux in arcjet facilities is the Gardon gauge shown schematically in Fig. 3. The principle on which heat flux is determined is that the temperature difference between the center and outer edge of the constantan disk is proportional to the heat flux. This temperature difference is sensed by a pair of differential thermocouples, one at the junction between the copper wire and the center of the disk, and the other at the junction between

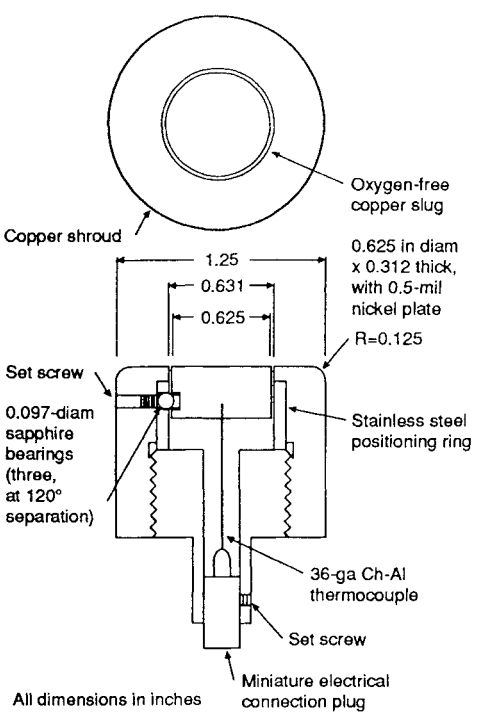

Fig. 2 Typical slug heat flux sensor.[4]

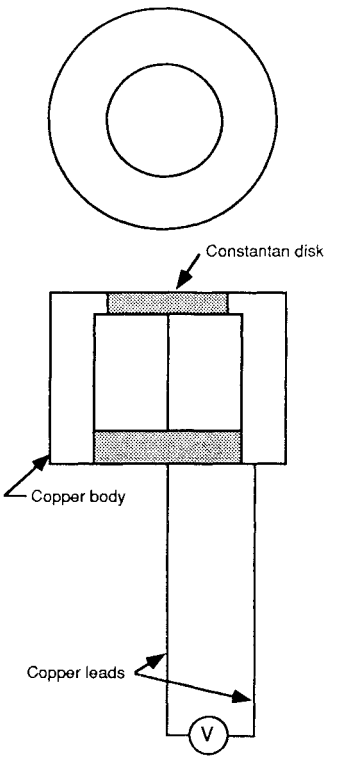

Fig. 3 Schematic of Gardon gauge heat flux sensor.

the outer edge of the disk and the copper body of the instrument. The output then can be calibrated with a suitable standard heat flux source, such as a blackbody. The sensitivity of the instrument is determined by the thickness of the constantan disk and its radius. These instruments are commercially available and come in various ranges. They may be water-cooled for continuous operation. One drawback to the Gardon gauge is its sensitivity to electrical noise generated by the arc. Therefore, care must be taken to electrically isolate its leads by shielding and to avoid ground loops. Another drawback to gauges that require calibration is that the calibration source is usually a radiant source, thus the radiant absorptance of the gauge must be known. Usually this is accomplished by coating the gauge with carbon black for the calibration. However, when using the probe in a dissociated nonequilibrium flow, the catalytic recombination rate of the surface must be known or it must be fully catalytic. This means that the probe surface must be carefully cleaned and have a coating of a material of known catalyticy. Frequently, the gauge is assumed to be fully catalytic, but that is only an approximation. Slug calorimeters avoid the problem of having to put on an overcoat of carbon black for calibration. These are transient devices, however, and they cannot be used continuously or for many insertions into the flow without allowing them to cool down.

Pressure Measurements and Estimates of Mass Fractions

The stagnation pressure probe is an intrusive diagnostic measurement commonly used in arcjet facilities to determine the uniformity of the flow. It is also used in conjunction with the heat flux probe to determine the enthalpy. The pressure is needed to verify that the flow regime simulates the appropriate conditions that depend on pressure. When in a stagnation test mode, the stagnation pressure drives the flow through any leak paths that may exist in the configuration. The stagnation pressure also can be used along with the bulk enthalpy (determined from, e.g., the energy balance method) and the gas flow rate to estimate the amount of dissociation.[11] This technique assumes that the flow is uniform and that the effective area of the nozzle or inviscid core is known. When a

single gas such as nitrogen is used the dissociation is found by a straightforward use of the conservation equations

$$h_T = \tfrac{1}{2}V_\infty^2 + \alpha_N h_N + C_p T_\infty \tag{7}$$

$$p_{T2} = \frac{C_P}{2}\rho_\infty V_\infty^2 + p_\infty \tag{8}$$

$$m_g = \rho_\infty V_\infty A_{\text{eff}} \tag{9}$$

The stagnation point pressure is p_{T2}, the pressure coefficient is C_P, C_P is the specific heat of the gas mixture, and A_{eff} is the effective area of the nozzle flow. These equations can be solved along with the equation of state and an estimate of the Mach number to find the atom mass fraction α_N. When the gas is air it has been assumed that either none of the nitrogen is dissociated and a set of equations analogous to Eqs. (7–9) is solved; or a term is included in Eq. (7) in which $\alpha_0 = 0.234$ (which is to say that all the oxygen is dissociated) and we solve for the nitrogen atom mass fraction α_N. If the enthalpy is low, then no nitrogen dissociation is assumed, and we solve for the oxygen mass fraction. Later it will be shown that these assumptions may not be valid. Clearly we need a way of determining the mass fractions directly. Such a method has been developed and will be discussed in the next section.

Mass Fractions from Gas Sampling Mass Spectrometer Measurements

An intrusive diagnostic technique is the use of mass spectrometer analysis of samples of flow drawn in from a stagnation point gas sampling probe. This technique may be used to directly determine the species concentrations in shock-layer flow. If the flow can be assumed to be frozen in the shock layer, then the technique can be used to determine the composition of the freestream flow. The first use in arcjets of such a probe, to the author's knowledge, was made about the same time in different facilities by Willey[12,13] and by Lasgorceix.[14] Willey applied the method to measure the relative concentrations of the constituents of air in a supersonic arcjet flow by sampling through a water-cooled quartz-tipped probe and a water-cooled copper probe adapted from a Pitot pressure probe. Figure 4 is a schematic of Willey's apparatus. He showed that it is necessary to make the probe from noncatalytic materials such as quartz and to make the length of the tube to the mass spectrometer as short as possible. He demonstrated that the concentrations of atomic species in the flow vary axially and radially, in contradiction with one-dimensional nonequilibrium flow calculations.[6,11] The contours of nitrogen atom concentrations in the vicinity of a blunt body inserted into the flow are shown in Fig. 5. Lasgorceix,[14] using a molecular beam mass spectrometer probe, also showed that the flow in their nitrogen jet was significantly out of equilibrium, but was not frozen. Figure 6 taken from Ref. 14 appears to show an increase in ionization fraction with distance, whereas the fraction of N relative to N_2 decreases, as seen in Fig. 7. These results contradict the assumption of frozen flow in low-density arcjet streams and indicate the need to directly measure these quantities when using arcjets for wall catalytic

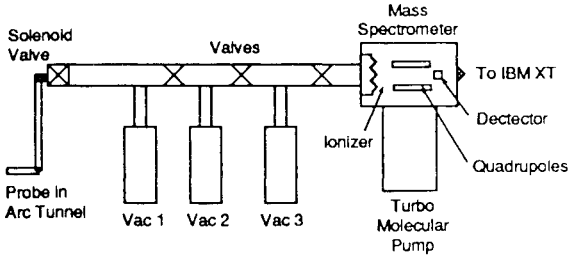

Fig. 4 Schematic of gas sampling probe used with mass spectrometer for species analysis.[12]

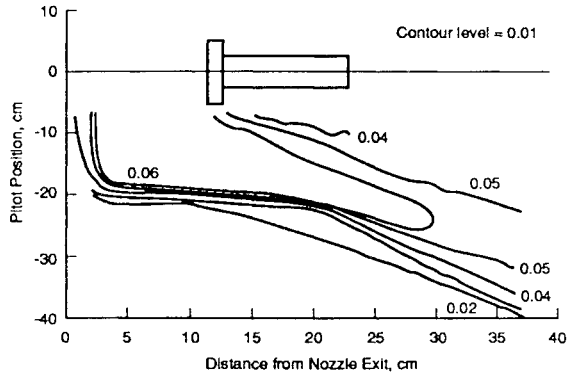

Fig. 5 Nitrogen atom concentration contours in arcjet flow around a blunt body.[12]

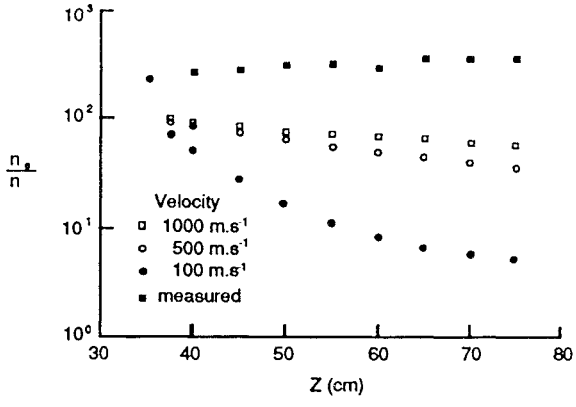

Fig. 6 Axial profile of the neutral particles ionization fraction N^+, and N in arcjet flow.[14]

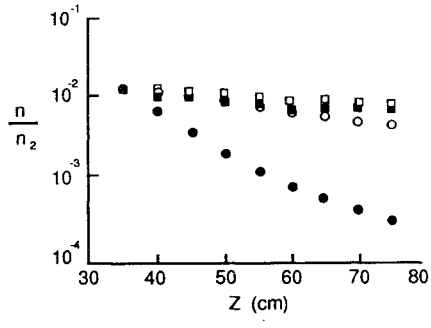

Fig. 7 Axial profile of dissociation fraction N/N_2 in arcjet flow.[14]

recombination measurements. Likewise, it may mean that gas-phase reaction rate models need significant refinement.

Gas Temperatures

The temperature of high enthalpy gases cannot be measured directly with a thermometer because the measuring device will perturb the gas. Indirect, nonintrusive means are almost always used. As shown in Table 1, there are several temperatures in a nonequilibrium flow, and many techniques are available, depending on which temperature is to be measured. The temperatures to be discussed are the molecular rotational and vibrational temperature, atom and molecule electronic state excitation temperature, the electron temperature, and the heavy particle translational temperature. Measurements of the radiation from the flow or laser light scattered by the flow constituents allow determination of these temperatures. Because these techniques involve the use of spectroscopy, a brief discussion of spectroscopic apparatus will be included first.

Because the enthalpy is very high, arcjet flows have a tendency to radiate spontaneously, especially in the shock layers. There is a lot that can be learned from the emission. However,

the freestream flow radiates much less, and not all excited states of species in the flow have spontaneous radiative transitions or have transitions in convenient wavelength ranges. Also there are limitations because of either detector response or overlapping radiation from other species or states. It would, therefore, be prudent to excite the species to radiate from specific states as a means of obtaining information about said states. Thus, state-selective laser-induced transitions are useful. Emission spectroscopy, and to some extent absorption spectroscopy, will be discussed in succeeding sections. Then, recent developments in laser-induced fluorescence applied to arcjet flows will be addressed followed by a brief discussion on the use of laser Thomson scattering to determine electron density and temperature in a plasma jet.

Spectroscopic Techniques

Two areas of spectroscopic techniques will be addressed here. The first is a brief description of apparatus and techniques for measuring the spectral radiation. Some older methods are described as well as modern techniques, including calibration sources. The other area of spectroscopic techniques is the interpretation of measurements with suitable theoretical methods. Interpretation of measurements is the main area of emphasis in this paper because it relates to both emission and absorption spectroscopy in addition to laser-induced fluorescence spectroscopy. Examples of techniques applied to arcjets will be given.

Spectroscopic Measurement Apparatus

Various emission and absorption spectral instruments have been used in arcjet facilities. These range from simple scanning monochromators to high-resolution grating spectrographs and spectrometers. The low-resolution monochromators have good light-gathering ability because of their short focal length and low F-number (ratio of focal length to aperture diameter). For high resolution it is necessary to sacrifice some light-gathering capability because the focal length of the devices must be long. In the 1960s a 3.4-m Ebert-type high-resolution spectrograph was commonly used.[15,16] Its F-number is about 22, but it can achieve a first-order dispersion of about 0.55 nm/mm with a grating ruled with 590 lines/mm. It covers a wide spectral range in one exposure.

The detectors used with spectrometers and monochromators are usually photomultiplier tubes that are sensitive to the wavelengths of interest. Response time is very fast, and an added advantage is that output can be recorded electronically for subsequent computer manipulation. In some spectrometers more than one photomultiplier can be used at a time to measure the light from several spectral lines. This requires using one exit slit and photomultiplier for each line.

To scan lines to determine line shape or to obtain a sequence of lines or the variation of continuum with wavelength, the grating may be rotated and a single detector can measure the spectrum as a function of wavelength, provided the source is not changing in time. If the region of the spectrum is large and high-resolution is required, this procedure may take a long time. Another method of obtaining a large wavelength range with high-resolution is to use a spectrograph with a photographic plate as the detector. Very high-resolution can be achieved with this technique because, with small-grain emulsions, the resolution is limited only by the entrance slit; whereas, the photomultiplier tube also requires an exit slit which somewhat degrades the resolution. Moreover, the spectrographic plates may be exposed for very long periods of time to achieve sufficient exposure to detect low-intensity spectra. The following are several difficulties encountered while using photographic detection: 1) the response is nonlinear and requires a densitometer to read the transmission of the plates to determine intensity; 2) development of the plate must be highly controlled, and the density of the plate must be carefully calibrated for quantitative work; 3) interpreting the results is very tedious; and 4) the sensitivity of photographic emulsions in the infrared (IR) is fairly low, requiring long exposures. However, the photographic recording of spectra is very good for yielding a comprehensive graphical picture of the spectral characteristics of the flow spectrum over a wide wavelength range.

Modern innovations for measuring spectra include using linear diode array (LDA) detectors. These devices have about 1000 detector elements covering a distance of about 25 mm. These LDAs can acquire 1000 pieces of spectral information simultaneously. They are then read out sequentially, digitized, and recorded by a multichannel optical analyzer (OMA) for computer data handling and analysis. The advantage of having many channels of data acquired simultaneously and repeatedly is that should the intensity of the source vary, all wavelengths will be affected to the same extent, and the relative intensity of the lines is not changed. The time dependence of the entire spectrum can also be obtained by gating the LDA. One disadvantage is that their resolution capability is somewhat limited but that can be overcome by selecting gratings with the appropriate blaze and ruling. You are then limited to the wavelength range that can be detected in a single "exposure."

Spectroscopic Measurement Calibrations

For quantitative work, spectrometers must be calibrated in both wavelength and intensity sensitivity. Wavelength calibration sources are usually gas discharge lamps filled with a gas that radiates with a well-known spectrum. These lamps may be excited with a high voltage source by way of electrodes in contact with the gas, or they are sometimes excited with a radio frequency (rf) electrodeless source. The electrodeless discharge has the advantage of operation at a lower temperature and pressure; therefore, their spectral lines are usually narrower, and they are less subject to contamination. The lamps with electrodes are simpler to use, may have higher intensities, and come in a variety of gases to provide a wide coverage of wavelength ranges. Another rather cumbersome source used for very fine wavelength definition is the iron arc. The iron arc spectrum contains thousands of closely spaced lines that have been well catalogued.[17]

Common sources for intensity calibration are the standard tungsten ribbon filament lamps.[18] These can be obtained with calibrations traceable to the National Bureau of Standards. These lamps are useful from the near uv to the near IR. For the vacuum ultraviolet, a pressure arc discharge or a carbon arc might be used.[19,20] For calibrating in the IR, globar sources and blackbody cavities[21] are frequently employed.

Determining Temperatures and Excited State Populations from Spectral Analyses

To determine information about the arcjet flow from the emitted or absorbed spectra, a theory is used that relates the measurements to some property of interest. Spectroscopic techniques actually measure the rate at which the gas emits light; i.e., the intensity. The intensity of an optically thin gas depends on two basic quantities: 1) the number of species per unit volume in the particular upper excited state; and 2) the probability that the species will make a transition to a lower state. The transition probability A_{ij} is primarily a property of the emitting species and is determined from quantum mechanical calculations or is measured. However, A_{ij} may depend slightly on the environment in which the species exists; that is, collisions and electric and magnetic fields may perturb the electronic energy states slightly and cause small deviations in the energy levels of the states and their associated transition probabilities. These are small effects, and except when there is an interest in line broadening, they usually can be neglected. Suffice it to say that transition probabilities (or oscillator strengths) are properties of the radiating species.

The radiation also depends on the number of species in a particular state and the transition probability. The radiation

emitted from a species in state "i" to state "j" is

$$E_{ij} = n_i A_{ij} h\nu_{ij} \tag{10}$$

where E_{ij} power radiated per unit volume. Equation (10) holds in general—equilibrium or nonequilibrium. When local thermodynamic equilibrium exists, the relative number of species in a particular excited state is given by the Boltzmann relation

$$\frac{n_i}{n_0} = \exp\left(\frac{-E_i}{kT}\right)\frac{1}{Q_e} \tag{11}$$

where n_0 is the number density of species in the ground state, n_i is the number density of species in the state i, and E_i is the energy of the state i relative to the ground state. Combining Eqs. (10) and (11), the emitted power corresponding to a transition in an equilibrium gas is then

$$E_{ij} = n_0 A_{ij} h\nu_{ij} \exp\left(\frac{-E_i}{kT}\right)\frac{1}{Q_e} \tag{12}$$

From the relative intensities of atomic lines, continuum, or within molecular bands, it is possible to determine the excitation temperatures. From absolute intensities, it is possible to obtain densities of the excited states and, in equilibrium, the total density of the species. These techniques will be discussed in the following paragraphs.

Atomic Line Diagnostics

The temperature or population of states can be obtained from intensities of atomic lines. Equation (12) can be written in terms of the oscillator strength f, which is proportional to the transition probability A_{ij}. I is given by

$$I = \frac{2\pi hc^2 r_0}{\lambda^3} gf \frac{n_0}{Q_e} \exp\left(\frac{-E_u}{kT}\right) \tag{13}$$

Equations (12) and (13) reveal that when the states are in equilibrium, a plot of the logarithm of the measured E_{ij} or I vs E_i/k will yield the excitation temperature from the slope of the plot $1/T$. If the population of states deviates from equilibrium then the points will not fall on a straight line.

Argon Lines

Shipley[16] has used this intensity-slope method to determine temperatures in the shock layer of a blunt body in an argon plasma jet flow. A Boltzmann plot of his measurements is shown in Fig. 8. Bowen[22] used the Balmer series of hydrogen to obtain a temperature distribution in a high-pressure underexpanded jet. Adock[23] measured the temperature on the centerline of the freestream of an argon plasma jet. He also used a simplification often made when equilibrium is assured. Only two lines (states) are measured, and the temperature is found from the ratio of intensities of the two lines.

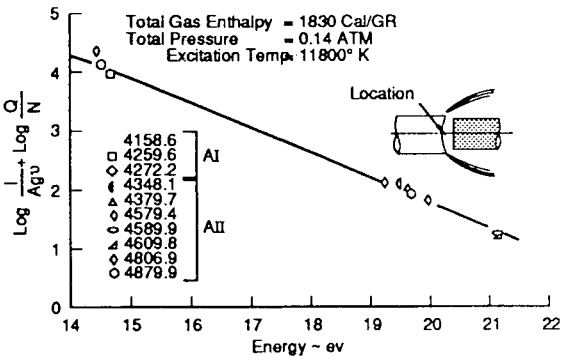

Fig. 8 Boltzmann plot of argon spectral lines. Both Ar I and Ar II lines are presented.[16]

Copper Lines

The line ratio technique has also been used for determining the excitation temperature in atmospheric arcjets using copper lines.[24] Copper from electrode erosion is a contaminant often found in arcjet flows. Recently, copper contamination has been exploited by a laser-induced fluorescence (LIF) Doppler technique; this is discussed in a subsequent section.

Nitrogen Lines

In air and nitrogen jets, nitrogen lines are sometimes used to determine the excitation temperature. Park[25] measured the electronic excitation temperature in a supersonic nozzle expansion that started from a stagnating inlet flow in a nitrogen-hydrogen mixture. The source of the flow was an arc heater. Park's nozzle was inserted in the arcjet flow. The measured temperature increased as the flow approached the converging part of the nozzle, then decreased as the flow expanded supersonically. The result was good agreement with flow theory calculations.

Helium Lines

Scott[15] determined the temperature profile of a helium arcjet flow using the line intensity technique. His results, using absorption oscillator strengths from Green et al.,[26] and energy levels of Martin,[27] are shown in Fig. 9. From these measurements, it was shown that the electrons were in equilibrium with the electronic states of helium.

Rotational and Vibrational Temperatures of Molecules

The rotational temperature and the vibrational temperature of molecules can be determined from the rotational and vibrational spectra of radiating molecules, either from emission or from scattered laser radiation. Usually emission is from excited electronic states of the molecule. Radiation from the electronic transitions is measured, and that radiation includes the information about the population of rotational and vibrational modes of energy. Therefore, a measure of the associated temperatures can be obtained.

Because of the complex configuration of electrons in molecules and the additional modes of energy, viz., the rotational and vibrational modes, molecular radiation is much more complex than atomic radiation. See Fig. 10 for an example of the visible radiation spectrum of a simple diatomic molecule—nitrogen. As can be seen, there are many complex band features that make up the spectrum. The rotational structure of these bands can be seen in highly resolved spectra and from the pattern of intensities the rotational temperature can be

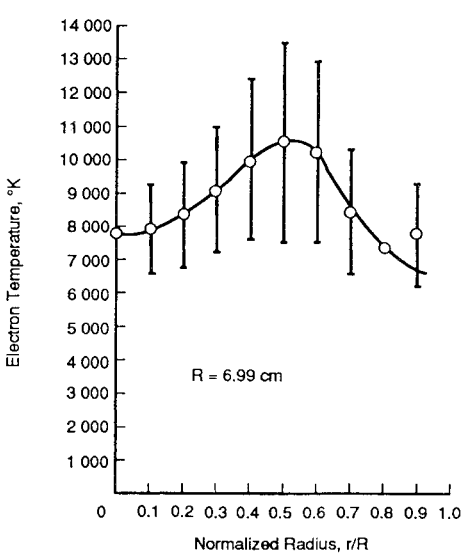

Fig. 9 Electron temperature distribution in helium arcjet flow, determined from Boltzmann plots. Error bars denote standard deviations.[15]

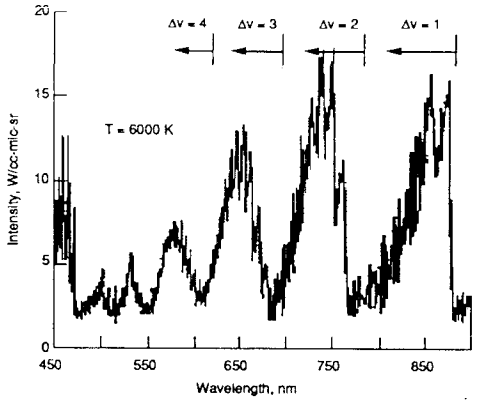

Fig. 10 Computed spectrum of N_2 for $T = T_v$ and $T_e = 6000$ K.[30]

obtained. Details of the theory of the spectra will not be covered except to point out that the intensities are determined from Eq. (12). The complexity arises from the form of the transition probability A_{ij} and the form of the energy E_i. The states i and j depend on many quantum numbers[28]; e.g., the electron spin, the orbital angular momentum, total angular momentum of the electrons, component of angular momentum along the internuclear axis, the rotational quantum number, and the vibrational quantum number. To use the radiation from even the simple molecule such as N_2^+, features of a complex spectrum must be isolated and studied to address one mode of energy, while keeping the others fixed. That is, if the intensity variation of the spectrum is addressed as a function of the rotational quantum number, the rotational temperature can be obtained. As before, a temperature is defined only if the energy levels are connected by a Boltzmann factor distribution. For rotation, which requires only 5–10 collisions to come to equilibrium, equilibrium usually exists in conditions of arcjet flows. On the other hand, vibration relaxes more slowly, requiring many more collisions. Therefore, vibrational states may be out of equilibrium, especially in the expanding low-density flow of arcjets and near shock waves, although the situation may be somewhat nearer vibrational equilibrium in the shock layer of a blunt body.

Molecules of interest in arcjets used for re-entry simulation are N_2, N_2^+, O_2, NO, and sometimes OH. Some examples of the use of molecular emission used as a diagnostic in arcjets are given in the following paragraphs.

N_2^+ (First Negative) System

The $B^2\Sigma_u^+ - X^2\Sigma_g^+$ transition of the N_2^+ molecule, is referred as the N_2^+ (first negative) system. One of the earliest examples of the rotational temperature determination in an arcjet flow is that of Shipley[16] who obtained the average rotational temperature in the jet freestream from the N_2^+ (first negative) bands, (0, 0) and (0, 1). His Boltzmann plot is given in Fig. 11 for the R and P branches of the (0, 0) band. Shipley was not able to use the technique in the shock layer of a blunt body because of other overlapping features of the spectrum and lack of spectral resolution.

Park[25] obtained the vibrational temperature in the stagnation region of the expansion nozzle by comparing the measured N_2^+ (first negative) spectrum with a calculated spectrum of Whiting et al.[29]

Recently the N_2^+ (first negative) spectrum was used to determine the vibrational and rotational temperature in the shock layer of a blunt body in a nitrogen arcjet flow at the Johnson Space Center. Blackwell et al.[30] fit the (0, 1) and (1, 2) bands to a computed spectrum[31,32] to obtain the rotational and vibrational temperature distribution. Examples of the spectra are shown in Fig. 12. Note that the computed spectrum has been fit very well to the measured spectrum as is evidenced by the fact that the curves overlap considerably. The resulting temperature profile is shown in Fig. 13. It can be seen that

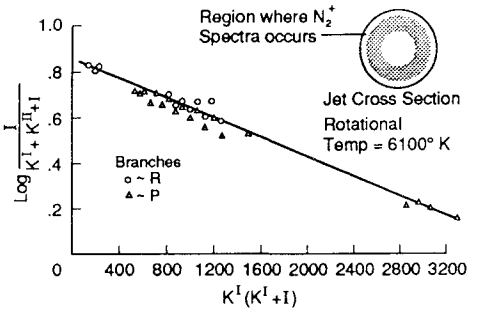

Fig. 11 Boltzmann plot of N_2^+ rotational lines from nitrogen arcjet.[16]

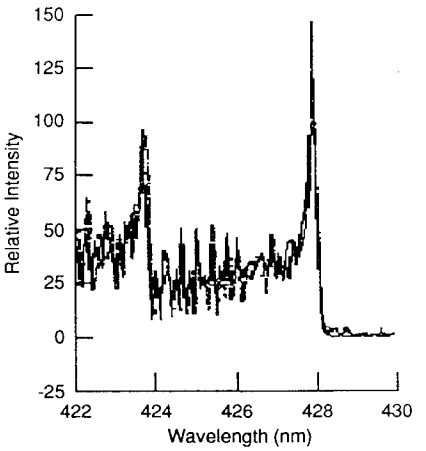

Fig. 12 Measured and computed spectra showing N_2^+ (first negative) (0, 1) and (1, 2) bands at 1.27 cm from surface.[30]

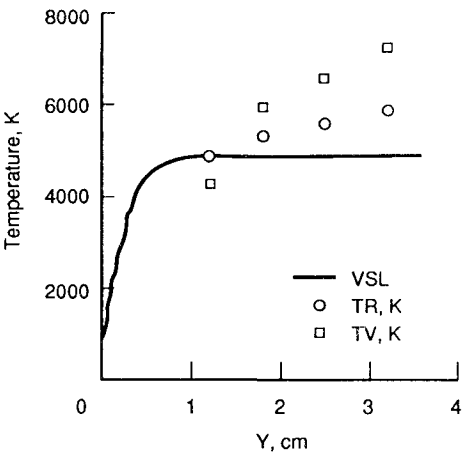

Fig. 13 Measured vibrational and rotational temperatures determined by spectral fitting compared with viscous shock layer single temperature calculation.[30]

the two temperatures are not equal, implying that there has not been enough time for the temperatures to relax to a common equilibrium temperature. The temperature computed by a viscous shock layer code,[33] shown in Fig. 13, was based on a single temperature gas model and cannot discriminate thermal nonequilibrium effects. The method of comparing the measured and computed spectra is required here, because the resolution of the spectrometer is not sufficient to resolve the rotational structure in which the R and P branches overlap.

The existence of a Boltzmann distribution of vibrational states was also checked by Blackwell et al.[30] The fits made by varying the relative population of the upper vibrational state indicated that the vibrational states of the N_2^+ (first negative) system deviate from equilibrium and that a vibrational temperature cannot be defined at all locations in the

shock layer. However, there was some evidence that overlapping bands may have caused some of this deviation.

N_2 (First Positive) System

A more difficult system to analyze than N_2^+ is the N_2 (first positive) system. Its transitions are between the $B^3\,\Pi_g$ and $A^3\,\Sigma u^+$ states for which there are many overlapping vibrational and rotational bands. Figure 10 shows the system where the broad peaks approximately correspond to regions of constant $\Delta v = v'' - v'$. Without an extremely high resolution spectrum, the only way to extract temperature information from this spectrum is to fit a computed spectrum to the measured spectrum. Blackwell et al.[34] compared the computed ratios of integrals of intensities in spectral regions with measured ratios to obtain vibrational and rotational temperatures. This procedure was applied to radiation from the shock layer of a blunt body in an arcjet airflow. More recently, Blackwell et al.[35] compared the vibrational and rotational temperatures of N_2 and N_2^+.

OH Spectrum

Water vapor from steam ejector vacuum systems or desorbed from surfaces sometimes contaminate the flow in arcjets. Also, OH may be produced in boundary layers around ablating test articles. Fishburne and Petrie[36] measured the rotational temperature distribution across an arcjet nozzle flow using OH as a diagnostic. They presumed that the OH is present as a trace species in the argon gas supply or is from minute leaks in the test chamber. To determine the rotational temperature, Fishburne and Petrie developed Boltzmann plots of the Q_1 branch of the transition ^2S-^2P (0, 0). Their temperature distributions are shown in Fig. 14. These results indicate that the flow is fairly uniform, but peaked slightly in the center of the jet.

Absorption Techniques

Many species of interest in arcjet flows do not radiate. For example, ground state atoms and molecules cannot radiate, and the transition probabilities of atoms and molecules in metastable states are very low. Therefore, these species do not emit appreciably. To determine the population of these ground and metastable states, one can do absorption measures. The transition probability for a transition from a lower state to an upper state is uniquely related to the transition from the upper to the lower state. Therefore, by illuminating the flow with radiation from a suitable source and measuring its attenuation through the gas, a measure of the population of the lower state can be obtained. Such an experiment was carried out by Valentin et al.[37] in an argon arcjet flow. They measured the metastable population distribution in the thermal boundary layer of a metallic flat plate, the surface of which was aligned parallel to the flow. The metastable density distribution is shown in Fig. 15. They also measured the population of electrons and the electron temperature distributions from the emission line intensities. They found that the population of the metastable and the other excited states was much larger than expected from equilibrium considerations. The excitation temperature profile in the boundary layer seen in Fig. 16 showed an unexpected increase near the wall when the boundary-layer edge temperature was low. Valentin et al.[37] postulated that the increase was due to ions colliding with the wall, causing Auger electrons to be ejected from the surface with an energy of a few electron volts which heated the boundary layer.

Laser-Based Techniques

Much information about the flow is available from emission spectra. However, the measurements are sums of the radiation along the line-of-sight of the spectrometer. If the flow is not uniform, the measurement results in an average over the line-of-sight; this is not a local quantity. To obtain local information from line-of-sight measurements of axisymmetric flows, the Abel inversion technique may be used. However, this technique is cumbersome and introduces some error into the results. Also, in many cases the flow does not have axial symmetry. Laser-based techniques can overcome the problem of line-of-sight averages, because the laser illumination can be focused along one line while the observation or measurement is made along a line orthogonal to the laser. Thus, the volume of gas formed by the intersection of the laser beam and the field-of-view is very small.

There are several types of laser-based techniques that have been used to measure properties in gases. These include Rayleigh scattering, coherent antistokes Raman scattering (CARS and BOXCARS), Mie scattering, stimulated Raman scattering, laser-induced fluorescence (LIF), and Thomson scattering. Of these techniques, only the last three have as yet been applied to arcjet flows. The LIF and Thomson scattering are discussed in the following paragraphs.

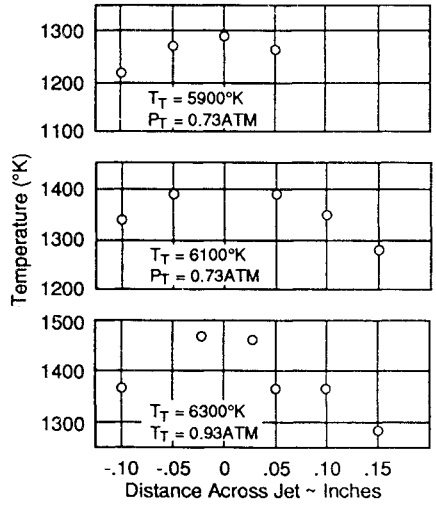

Fig. 14 OH rotational temperature distribution across core of exhaust jet.[36]

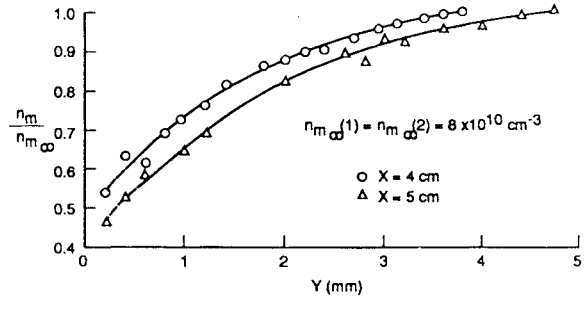

Fig. 15 Argon metastable density profiles in the boundary layer of a flat plate.[44]

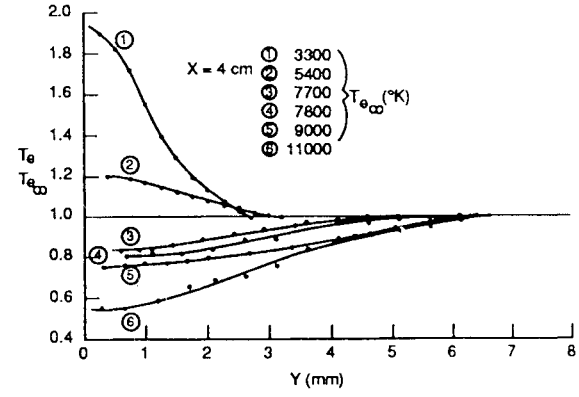

Fig. 16 Electron temperature profiles in the boundary layer of a flat plate with various freestream temperature conditions.[37]

Laser-Induced Fluorescence

When molecules or atoms are illuminated with radiation having frequency that corresponds to a transition between states, the species may absorb the radiation and subsequently emit the energy to allowed lower states. Examples of such transitions are shown in Fig. 17.

The rate at which the upper state is formed depends on the density of molecules in the lower state n_l, the absorption transition probability A_{lu}, and the intensity of the laser I_L, and the energy per photon $h\nu_{lu}$:

$$\frac{dn_u}{dt} \propto \frac{n_l I_L A_{lu}}{h\nu_{lu}} \tag{14}$$

As in the case of spontaneous emission, the amount of radiation that is emitted from the excited molecule is proportional to the emission transition probability A_{ul} from upper state u to each lower state l. The loss of upper state molecules due to radiation and collisions is given by

$$\frac{dn_u}{dt} = \sum_j n_u A_{uj} + n_u \nu_u \tag{15}$$

where n_u is the number density of molecules in the upper state and ν_u is the collision frequency for de-excitation. Equations (14) and (15) can be solved to determine various properties of the flow, depending upon what is known. If the only source of excitation is the laser radiation and the radiative lifetime of the excited state is short compared with the collisional lifetime (or $A_{uj} >> \nu_u$), then the measured intensity of the emitted radiation will yield the density of the lower state. In the case of molecules, the laser wavelength can be tuned so that the density of the lower states is determined. Thus, as in the case of absorption, the excitation temperature of the molecules' lower states now can be obtained without the complication of overlapping bands and with the advantage that the measurement is local.

A variety of wavelength ranges is possible using various types of lasers, dyes, and doubling/mixing crystals. Therefore, LIF access is available for diagnosing many molecules and transitions.

Arepalli[38] demonstrated the ability to obtain LIF signals from NO and O_2 in the freestream and shock layer of an arcjet at NASA Johnson Space Center. He produced a tunable (approximately 226 nm) uv laser signal using the 355-nm wavelength line of the pulsed YAG laser to pump a tunable dye laser which had an output of about 430–470 nm. The wavelength of the output beam was halved to about 225 nm, using a crystal doubler. The output power in this range was about 1.2 mJ, and the bandwidth was 0.01 nm. The LIF signal from the flow zone was measured with a photon-counting photomultiplier gated to reduce background radiation from the flow. Filters in front of the photomultiplier restricted the spectrum to pass only light from specific species. The optical arrangement is shown in Fig. 18. Preliminary results indicate that at low enthalpy NO and O_2 are readily detectable. The corresponding energy levels and the transitions studied are shown in Fig. 17. By tuning the output of the laser, the various NO ground electronic state vibrational levels $X^2\,\Pi_{1/2,3/2}$ could be excited to the upper states $A^2\,\Sigma^+$. The fluorescent signals from the upper states were then measured with a wide band photomultiplier. Sample NO spectra are shown in Fig. 19 obtained in the freestream with filters in place to detect the NO $A^2\,\Sigma^+ — X^2\,\Pi_{1/2,3/2}$. It can be seen from the three scans that as the enthalpy increases, the NO LIF signal decreases. This is consistent with the decrease in NO at higher temperatures.

Arepalli[38] also obtained LIF signals for the O_2 Schumann-Runge transitions $B^3\,\Sigma_u^- — X^3\,\Sigma_g^-$ $(v', v'') = (0, 3)$, $(2, 4)$, and $(4, 5)$. Induced fluorescent transitions back to the X state were measured with a 225–540-nm filter. Arepalli expects to obtain vibrational and rotational temperatures and densities of the ground state in the near future from LIF spectra.

Laser Raman Scattering

Laser Raman scattering involves an inelastic scattering of light from species that results in a molecularly specific fre-

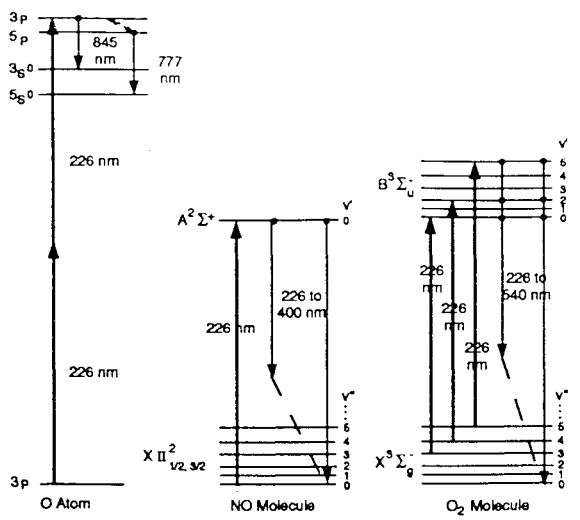

Fig. 17 Energy level diagrams for O, NO, and O_2.[38]

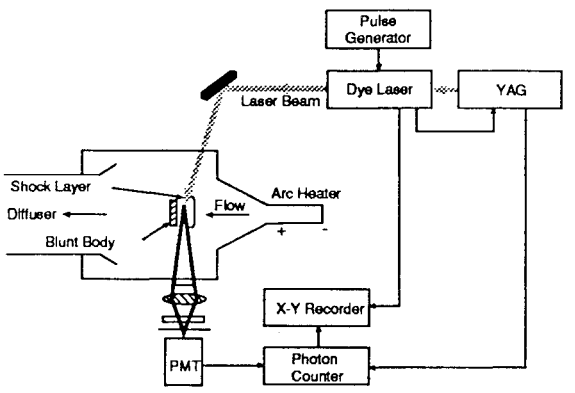

Fig. 18 LIF experimental setup.[38]

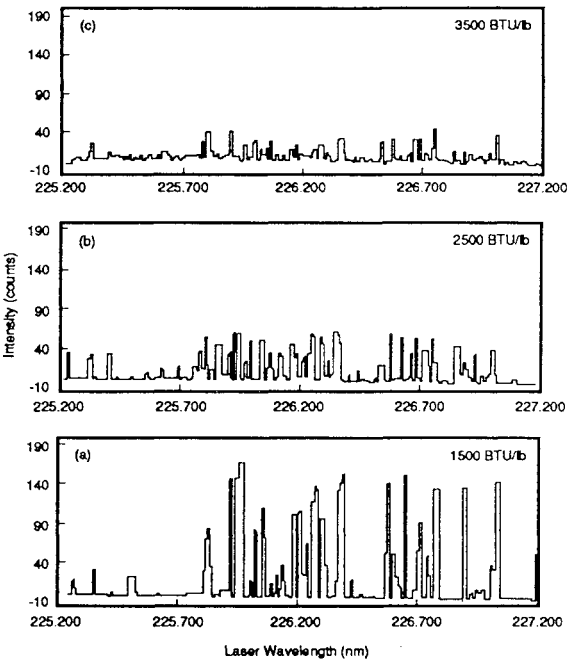

Fig. 19 LIF spectrum of (0, 0) band of NO (A-X) in freestream of arcjet under three enthalpy conditions.[38]

quency shift of the scattered light relative to the frequency of the incident beam. The frequency spectrum depends on the energy states of the scattering species; therefore, the spectrum of the scattered light is determined by the population of states in the scattering molecule. It can probe the spectrum of states inaccessible by emission spectroscopy, resulting in a detectable scattered signal that has the spectral signature of, e.g., the ground electronic state molecule. Boiarski and Daum[39] have studied the feasibility of using laser Raman scattering for measuring number densities and vibrational temperature of nitrogen, oxygen, and nitric oxide. Their exploratory experiments in the Air Force Flight Dynamics Laboratory 50-Megawatt Reentry Nose Tip (RENT) facility have shown the feasibility of the technique for arc tunnel flow diagnostics.

Translational Temperature of the Gas

The translational temperature of the gas can be measured directly with a Doppler technique by LIF of gas atoms or molecules in the flow. Very high resolution spectra from narrow laser lines are obtained by scanning a tunable laser over an isolated line of some species in the flow. This technique was first used in an arcjet by Arepalli et al.,[40] who scanned a copper line to obtain the velocity from the shift of the line and the temperature from the Doppler profile. The Doppler shift of light relative to the moving atom is given by the familiar relation

$$\frac{\Delta\nu}{\nu_0} = v/c \tag{16}$$

where v is the relative velocity of the particle with respect to the laser propagation vector. A moving atom whose resonant frequency is ν_0 will absorb a photon if the photon frequency is shifted by the Doppler frequency

$$\nu = \nu_0 + \Delta\nu$$

$$\nu = \nu_0 + (v/c)\,\nu_0$$

Because atoms have a random thermal velocity distribution, they will absorb laser energy provided the laser is tuned to coincide with the resonant Doppler frequency. The atoms subsequently fluoresce to some lower level at the characteristic frequency of the transition (which is detected by a photomultiplier). The number of photons emitted is proportional to the number of atoms whose velocity component in the laser propagation direction corresponds to the Doppler shifted frequency. Therefore, by scanning the laser's frequency, a profile of scattered light that corresponds to the velocity distribution can be obtained. For a Maxwell-Boltzmann velocity distribution, the line relative intensity profile is Gaussian and is given by

$$\frac{I(\nu)}{I(\nu_0)} = \exp\left[\frac{-mc^2}{2kT\nu_0^2}(\nu - \nu_0)^2\right] \tag{17}$$

For temperature measurements the laser may be beamed normal to the flow direction, and the scattered light may be observed from any convenient direction, assuming the velocity distribution is isotropic.

The Arepalli et al.[40] scan of copper resulted in broadened peaks associated with the laser's inability to resolve the fine structure of the line. By suitable fitting (such as a least squares fit of the measured profile to the theoretical line structure), the temperature and the splitting frequencies can be obtained. The optical arrangement is shown in Fig. 20 where it can be seen that the laser crosses the flow diagonally (in this case 30 deg) to obtain a component of the propagation vector in the flow direction. The fluorescent emission is observed normal to the jet flow direction. A sample copper line profile is given in Fig. 21 that corresponds to a temperature of 1000 K. The Doppler profile technique depends on other broadening

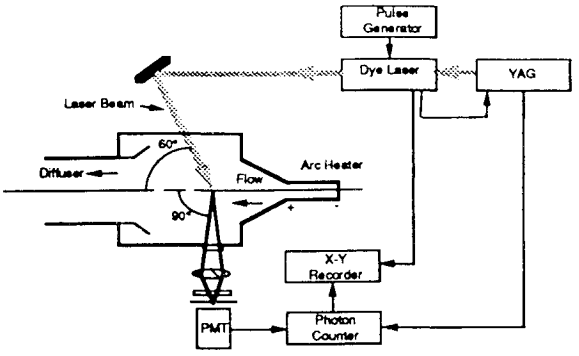

Fig. 20 LIF Doppler velocity and temperature measurements.

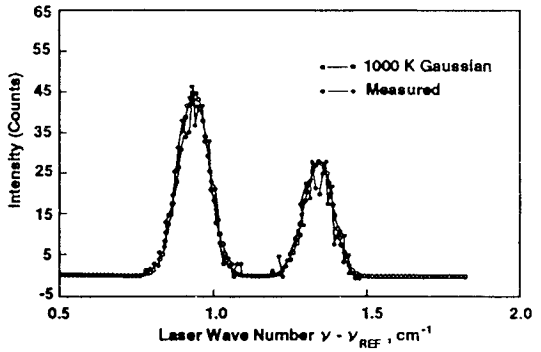

Fig. 21 LIF Doppler profile of copper transition.

mechanisms, such as Stark broadening, being negligible, which is frequently the case for most atoms other than hydrogen and helium in low-pressure arcjet flows. Likewise, the laser power must not be too high in order to avoid power broadening.

A discussion of determining the mean flow velocity will be presented in a subsequent section.

Electron Beam Fluorescence

The electron beam fluorescence technique can be used to determine the density of species in the ground state. It can also be used to determine the distribution of vibrational and rotational excited states, and thus the corresponding temperature. The technique is similar to LIF, but requires measuring the spectrum of the fluorescent emission rather than just the total emitted light which depends on a scanning of the incident laser in LIF. At moderate and low pressures an electron beam of several tens of kilovolts is passed through the flow, exciting the molecules and atoms. The radiation from the fluorescent emitting species is collected by a spectrometer and dispersed to obtain its spectrum. From analysis of the spectrum as described in the emission section, one can determine the species concentrations and the vibrational and rotational temperatures of molecules. The density of the flow must be low enough so that collisional quenching does not affect the density results. Application of the electron beam technique to arcjet flow diagnostics was developed by Petrie,[41] Sebacher,[42] Petrie and Lazdinis,[43] Lazdinis and Carpenter,[44] and Petrie.[45]

Some of the difficulties in using this technique to determine the species density are the problems of quenching, beam attenuation and scattering, accuracy of the excitation efficiencies, and geometry of the collection optics. A good calibration source is needed.

A measure of the flow velocity can be obtained by measuring the time of flight of electron perturbations produced by a modulated electron beam. The electron density perturbations are detected by electrostatic probes downstream of the beam. Cason[46] measured the velocity in an arcjet facility by this technique (adapted from a technique used in a helium afterglow by Trochan[47]). The measurements agreed with flow calculations within about 10%.

Electron Temperature and Electron Density

The electrons are usually not in equilibrium with the heavy particles in a low-density arcjet flow. Therefore, it is necessary to determine their temperature separately. Three techniques will be discussed in the sections that follow. Which technique that can be used usually depends on the electron density. Two of these are nonintrusive techniques for the measurement of electron temperature and electron density. The third is an intrusive technique. At moderate electron densities between about 10^{12}–10^{14} cm^{-3}, an emission continuum intensity method can be used. At very high densities, say above about 10^{14} cm^{-3}, laser Thomson scattering can yield the Doppler profile and, from that, the electron temperature. At low-electron density, an intrusive technique, electrostatic (Langmuir) probes, must be used. Microwave transmission techniques have been attempted, but that technique has poor spatial resolution and will not be discussed here.

Continuum Emission

The continuum radiation arises from transitions from free electrons to either bound states or to free states; this is called Bremstrahlung radiation. The intensity distribution of the continuum radiation depends on the electron temperature. The level of radiation depends on the electron density. Scott[15] determined the electron density in a helium arcjet using the relation[48] for the continuum emission coefficient

$$\varepsilon(\lambda,T) = \frac{K}{\lambda^2}\left[\frac{n_1}{n_i}\sum\frac{g_{nl}(\lambda)}{n^3}\exp\left(\frac{E_\infty - E_{nl}}{kT}\right) + \sum\frac{g_n(\lambda)}{n^3}\exp\left(\frac{E_H}{n^2kT}\right) + \frac{gf(\lambda,T)kT}{2E_H}\exp\left(\frac{\Delta E}{kT}\right)\right] \times n_e n_i \exp\left(-\frac{E_\lambda + \Delta E_\infty}{kT}\right)\left(\frac{E_H}{kT}\right)^{3/2} \quad (18)$$

where K is a combination of physical constants (see Ref. 49), n is the principle quantum number, E_H is the ionization potential of hydrogen, n_1/n_i is the ratio of ion ground state population to total ion population (set equal to 1), E_∞ is the ionization energy, E_{nl} is the excitation energy of the level, ΔE is the advance of the series limit, ΔE_∞ is the reduction in ionization energy, and the g are appropriate Gaunt factors. Because the flow is assumed to be electrically neutral ($n_e = n_i$), we can calculate the density from Eq. (18) and the measured continuum intensity

$$n_e = \sqrt{\frac{I(\lambda)}{\varepsilon(\lambda)}} \quad (19)$$

where $I(\lambda)$ is the measured power radiated per unit volume per steradian per unit wavelength at a point in the flow.

Scott[15] determined the electron density distribution from Abel inverted helium continuum measurements using Eqs. (11) and (19) and the electron temperature shown in Fig. 9. The density profile is shown in Fig. 22.

Doppler Laser Thomson Scattering

Free electrons have a fairly large photon scattering cross section. Based on the scattering cross section, the electron density can be determined by measuring the absolute scattered intensity. The electron temperature can be obtained from the profile of the scattered line. The (Doppler) intensity distribution of laser light scattered from a Maxwellian distribution of electrons is given by the relation[50]

$$I(\nu) = \frac{n_e r_e I_0 \sin\theta}{\nu_0^3}\exp\left[\left(\frac{\nu - \nu_0}{\delta\nu}\right)^2 / 2\right] \quad (20)$$

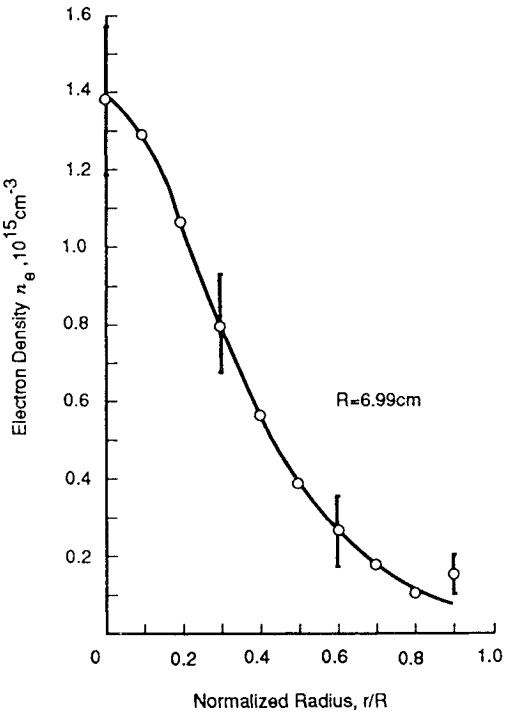

Fig. 22 Electron density distribution in helium arcjet flow. Error bars denote standard deviation.[15]

where I_0 is the laser intensity, ν_0 is the wave number of the laser, ν is the wave number of the scattered light, and $\delta\nu$ is the half-width at half-maximum of the measured line profile. Note that the scattered intensity varies inversely as the cube of the wave number, which means that the scattering is more efficient at long laser wavelength.

The temperature of the electrons can be determined from the Doppler width of the scattered laser line provided the electron velocity distribution is Maxwellian. In a continuum flow, a Maxwellian distribution is almost assured. The temperature of the electrons is given by the expression

$$T = \frac{m_e c^2}{2k}\left(\frac{\delta\nu/\nu_0}{2\sqrt{\ln 2}}\right)^2 \quad (21)$$

where m_e is the mass of the electron, $\delta\nu$ is the full width at half maximum, and ν_0 is the central wave number of the laser line.

The only known experiment in which Thomson scattering is used in arcjet flow diagnostics is that of Michels et al.[51] in which they measured temporal and radial profiles of electron density and temperature in a pulsed MPD arc thruster. Their apparatus is shown in Fig. 23. They found that the average density (in the range of about 10^{14} cm^{-3}) is rather constant over 100 μs but fluctuated significantly. Likewise, the average electron temperature which was in the range of about 4 eV was also fairly constant. The radial profiles were relatively flat at 4 cm from the nozzle exit.

Thomson scattering—most useful at high n_e—requires that the background scattered light be eliminated with the use of beam dumps and baffling. The Rayleigh scattered line, which is due to scattering from atoms and molecules and appears at the center wavelength of the Thomson scattered line, must also be filtered out by efficient and very narrow bandpass filters so no significant background light will be allowed into the detection spectrometer.

Electrostatic (Langmuir) Probes

Electrostatic probes are conductors in contact with the flow to which a positive or negative bias voltage is applied. The current collected, due to flux of electrons or ions, is measured

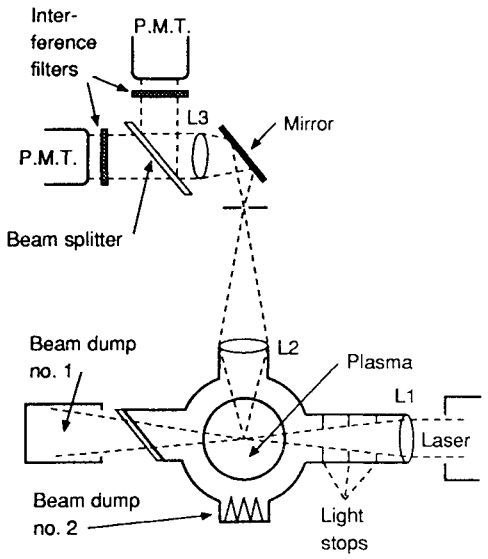

Fig. 23 Schematic of Thomson scattering diagnostic equipment.[51]

as a function of the applied voltage. If the probe circuit is left open it will acquire a potential (called the floating potential) that results in a net zero current. The flux of ions and the flux of electrons balance each other and the net flux is zero. To acquire this floating potential, the probe will have a net negative charge on it such that the electrons, which are much more mobile than the ions, will be repelled and the ions will be attracted in a way that will make the net fluxes equal. As the probe bias is made more negative it will collect more ions than electrons. At large negative bias the probe will reach what is called ion saturation; i.e., no more ions can reach the probe because they cannot diffuse fast enough into the "sheath" surrounding the probe. The sheath is a region in which there may be charge separation and the plasma is no longer neutral. The sheath thickness depends on the applied potential and arcjet conditions. Where the electron density is relatively high ($>10^{10}$ cm^{-3}), the sheath is often very thin with respect to other dimensions in the flow, including the mean free path. In the thin sheath case, we say that the sheath is collisionless, making the analysis much simpler. As the probe bias is made more positive the probe will collect more electrons and, at sufficiently high potential, will reach its electron saturation current. In analogy with the ions, the electron current saturates when the diffusion of electrons into the sheath no longer can keep up with their collection by the probe. Since the electrons are so light, and therefore, have a much higher thermal velocity compared with the ions, the electron saturation current is orders of magnitude larger than the ion saturation current.

In the transition zone between ion saturation and electron saturation, the net current depends strongly on the bias voltage and on the electron temperature. The slope of the logarithm of the current as a function of bias voltage is proportional to the inverse of the temperature, that is

$$\log (J_+ + J_-) = \log J_- - \frac{1}{T_e}\frac{eV}{k} \tag{22}$$

where $J_{+,-}$ are the ion and electron current densities, T_e is the electron temperature, and V is the bias voltage. We see that the temperature can be determined from the slope. The reason the slope of this equation decreases with increasing electron temperature is that more of the electrons have velocity (energy) great enough to overcome the negative bias of the probe, and therefore, the probe is able to collect more electrons (J_-) at large negative bias.

The electron and ion saturation current densities in a stationary plasma are respectively

$$J_- = \frac{n_e e}{4}\sqrt{\frac{8kT_e}{\pi m_e}} \tag{23}$$

$$J_+ = 0.4 n_i e \sqrt{\frac{2kT_e}{\pi m_i}} \tag{24}$$

T_i is assumed equal to T_e here.

Electrostatic probes also measure the electron and ion concentrations as well as the electron temperature, and they may be used to determine the flow velocity. Electrostatic or Langmuir probes are not used frequently in arcjet diagnostics. This is probably due to the degree of difficulty in building probes that will not disturb the flow and that will survive the high heating and oxidizing environment. Also, the theory of the probes often requires information about the flow; (e.g., the density, velocity, etc.) that may not be known or must be determined by other means. However, this technique may reveal much information about the spatial distribution of ions in the flow and the electron temperature that can be used with spectroscopic information to assess the rate of formation of species excited by electrons. If the flow is static or the flow velocity is much less than the random thermal velocity of the ions and electrons, then static probe theory can be used to analyze the current to the probe.

Water-cooled conical probes and uncooled cylindrical probes found use at the Langley Research Center.[52] (See Fig. 24, where a conical probe design is shown.) Electrostatic probes have been used in arc-generated argon plasma jets[53,54] and also in air[52] and nitrogen.[52,55,56]

Line (Stark) Broadening

When atoms or molecules undergo collisions with neighboring ions and electrons, their energy levels are perturbed by the electric fields of their neighbors. This results in the wavelength of the radiation from the excited species being shifted by the amount of the perturbation energy. Because the interactions are at various distances or strengths, the collection of species radiates at wavelengths that may cover a fairly wide range relative to their natural line width. The result is a broadened line, the width of which depends on the density of perturbing neighbors and somewhat on the temperature of the plasma. This Stark broadening phenomenon can be used as a diagnostic to determine the electron and ion density in the flow. Griem[49] presents tables of line-broadening data for a large number of species.

H and He Line Broadening

Because line widths of hydrogen and the diffuse series of helium are very broad, these species can be used for measuring fairly low-electron densities. Line broadening of hydrogen Balmer lines, H_α and H_β in arcjets was used to determine the electron (ion) density in Park's[25] experiments. Using line width data from Griem,[49] Park got good agreement with his flow theory[57] in the throat sections of the nozzle and reasonable agreement in the expansion section. His results are shown in Fig. 25.

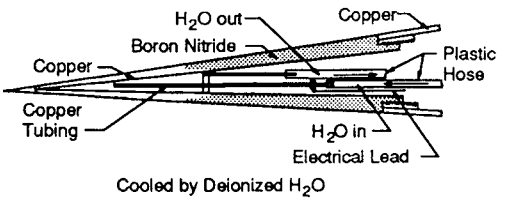

Fig. 24 Conical water-cooled electrostatic probe for arc service.[52]

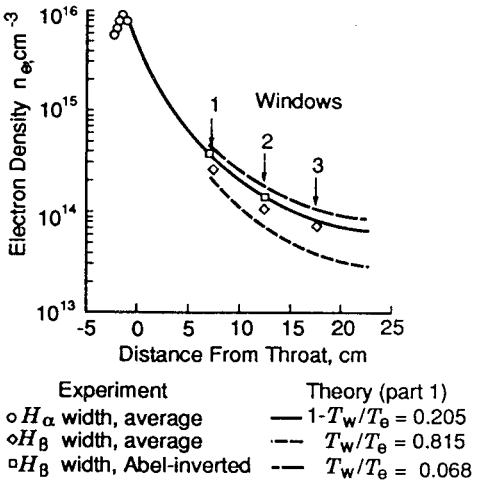

Fig. 25 Variation of electron density in nozzle.[25]

Scott[15] developed a quasistatic theory of line broadening of helium triplet diffuse lines (2^3P-n^3D transitions) and compared these results with measurements in a pure helium arcjet expansion flow. The electron density used in the calculations was determined for continuum measurements discussed in a previous section.

N and Ar Line Broadening

At higher electron densities, nitrogen and argon line broadening may be useful. In general, however, fairly high resolution instrumentation must be used to obtain electron densities using line broadening in low-density arcjets. Nitrogen and argon must normally be used with atmospheric pressure plasmas and not with low-density arcjets.

Flow Velocity

The velocity of the flow has been a very difficult property to measure in arcjets because of the high resolution required from spectroscopic means and difficulties with electrostatic probes. However, emission spectral techniques, laser induced fluorescence, and electrostatic probes have been used to measure velocities in arcjets and are discussed in the next three subsections.

Emission Doppler Shift Technique

Emission techniques usually suffer from lack of spatial resolution but have been used in MPD arcjet diagnostics for many years. For example, Beth and Kling[58] used a spectroscopic emission technique by using a Fabry-Perot interferometer to measure the Doppler shift of argon ion lines. By suitable Abel transformation they were able to obtain velocity profiles of the longitudinal velocity as well as the rotational velocity component. These methods have been developed and used along with the LIF Doppler technique which is also used to determine the kinetic temperature discussed previously. In addition, Doppler shift of the Thomson scattered laser light can be used to determine the velocity.

Laser-Induced Fluorescence Doppler Velocity Measurements

At high pressures, laser Doppler anemometry has been a popular technique for determining velocities in wind-tunnel flowfields. However, this particle scattering technique has several drawbacks for arcjet application. In particular, at high temperatures the seed particles may ablate and subsequently change size, and the velocity in arcjets is much higher than conventional wind tunnels, requiring very high frequency response detection systems. The LIF has been used successfully in wind tunnels and shock tubes to determine velocity, and recently the technique described for determining the Doppler

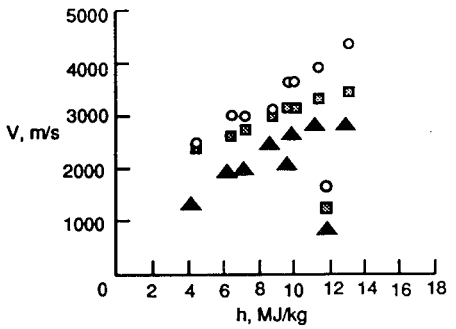

Fig. 26 Measured and calculated arcjet centerline velocity.

temperature in arcjets has been used for determining velocities.[38]

As mentioned in a previous section, the relative Doppler shift of radiation equals the velocity component in the propagation direction divided by the velocity of light. By beaming a laser through a flow so that its propagation direction has a significant component in the flow direction, the velocity can be calculated from the relation

$$\frac{v}{c}\cos\varphi = \frac{\Delta\nu}{\nu} \tag{25}$$

Arepalli et al.[40] measured the centerline velocity at a point downstream of the nozzle exit at several flow conditions. Their results are shown in Fig. 26, where calculated velocities are compared with the measurements. It can be seen that the measurements are about 25–50% lower than the calculations, indicating that assumptions used in the calculations are probably in error and that detailed diagnostic measurements and calculations need to be made.

Electrostatic Probe Velocity Measurements

Velocities have also been measured in low-density argon and nitrogen arcjet flows by Poissant and Dudeck.[54] They used flat-tipped probes having the exposed electrode flush with the ends of the probes. Two probes were inserted into the flow: 1) one oriented parallel to the flow direction; and 2) the other perpendicular to the flow direction. The ratio of the currents drawn by the probes was a measure of the flow velocity since the current collected by a negatively biased probe—the surface of which is normal to the flow—is given by

$$I_- \approx n_i v A \tag{26}$$

where A is the probe area. This relation applies if the flow velocity is large compared with the thermal velocity and for free molecule flow. The current to the other probe I is given by Eqs. (23) and (24), depending on its bias.

Other relations in a fairly extensive literature are available for probe currents in continuum flows, but they are more complicated. Such is the case in seeded combustion flows where electrostatic probe techniques have been used more extensively than in arcjets.

Conclusions

Determining the flow properties in arcjets still remains a difficult task. However, there are many diagnostic techniques available, and they have to be used in a complementary way to determine as much information as required. Even though the intrusive techniques disturb the flow, they have proved useful in giving much needed information about the flow. Determining the total enthalpy still remains a significant challenge. Accurate heat flux measurements require knowledge of atom recombination and chemical energy accommodation coefficients as well as enthalpy. With attention given to eliminating small errors and taking all pertinent physics into ac-

count, good estimates of the total enthalpy distribution in the flow can be made. The recently used modern technique of mass spectrometry appears to hold a lot of promise in revealing information about the species and chemical nonequilibrium in the flow.

The recent application of laser techniques for velocity and temperature determination promises to provide much needed direct validation of computer codes used to simulate the flow. These measurements will also be invaluable in determining the enthalpy of the flow and in determining atom fractions.

State specific methods, such as the spectroscopic and laser techniques, will find great utility in understanding the chemistry and nonequilibrium reaction rates and excitation rates in the flow. These rates and species concentrations are necessary for catalysis measurements and for determining the effects of atom recombination on surfaces.

The little used method of laser Thomson scattering has been included for completeness. This technique may find more use at very high enthalpy, e.g., in flows required to simulate very high-speed re-entries such as those associated with lunar or Mars missions.

This review article has not addressed the accuracy of the measurements nor the merit of one technique over another. It is premature to make such evaluations because many of these techniques are just now being used, and there have been few standards established by which to judge them. As these techniques are applied to a specific facility and a set of conditions consistent with each other and with high-fidelity calculations, they should yield better information upon which to assess accuracy of the techniques.

References

[1]Pope, R. B., "Measurements of Enthalpy in Low-Density Arc-Heated Flows," *AIAA Journal*, Vol. 6, Jan. 1968, pp. 103–110.

[2]Winnovich, W., "On the Equilibrium Sonic-Flow Method for Atmospheric Re-Entry Research," NASA TN D-2132, 1964.

[3]Shapiro, A. H., *The Dynamics and Thermodynamics of Compressible Fluid Flow, Vol. 1*, Ronald Press, New York, 1953.

[4]Hiester, N. K., and Clark., C. F., "Feasibility of Standard Evaluation of Procedures for Ablating Materials," NASA CR-379, 1966.

[5]Fay, J. A., and Riddell, F. R., "Theory of Stagnation Point Heat-Transfer in Dissociated Air," *Journal of Aerospace Sciences*, Vol. 25, 1958, pp. 73–85.

[6]Bade, W. L., and Yos, J. M., "The NATA Code—Theory and Analysis," NASA CR-2547, 1975.

[7]Boison, J. C., and Curtiss, H. A., "An Experimental Investigation of Blunt Body Stagnation Point Velocity Gradient," *ARS Journal*, Vol. 29, 1959, pp. 130–135.

[8]Scott, C. D., "Measured Catalycities of Various Candidate Space Shuttle Thermal Protection System Coatings at Low Temperatures," NASA TN D-7113, 1973.

[9]Scott, C. D., "An Experimental and Analytical Study of Slip and Catalytic Boundary Conditions Applied to Spheres in Low Reynolds Number Arc Jet Flows," *Rarefied Gas Dynamics, Proceedings of the Ninth International Symposium*, edited by M. Becker and M. Fiebig, DFVLR, Porz-Wahn, Germany, 1974, pp. D.14-1–D.14-12.

[10]Li, C.-P., "Numerical Solution of Viscous Reacting Blunt Body Flows of a Multicomponent Mixture," AIAA Paper 73-202, New York, Jan. 1973.

[11]Scott, C. D., "Catalytic Recombination of Nitrogen and Oxygen on High Temperature Reusable Surface Insulation," edited by A. L. Crosbie, Vol. 77, Progress in Astronautics and Aeronautics, AIAA, New York, 1981.

[12]Willey, R. J., "Direct Measurements of Atomic and Molecular Concentrations in Boundary and Surface Layers of Shocks," Northeastern Univ., Final Rept. Grant NAG 9-260, Boston, MA, March 13, 1989.

[13]Willey, R. J., and Blake, D. J., "Gas Composition Measurements in Arc Jet Tunnels via Mass Spectrometry," *Journal of Thermophysics and Heat Transfer*, Vol. 5, 1991, pp. 150–156.

[14]Lasgorceix, P. M., "Mise au Point d'un Ensemble Experimental d'Analysé de Jets de Plasma d'Arc Rarefiés. Application à un Jet de Plasma d'Azote," Ph.D. Dissertation, Université de Paris-Sud, Orsay, France, April 26, 1989.

[15]Scott, C. D., "Line Broadening of the Triplet Diffuse Series of Helium in an Arc-Jet Plasma," NASA TM X-58050, 1970.

[16]Shipley, K. L., "Some Spectroscopic Measurements of a Supersonic Plasmajet," *Applied Spectroscopy*, Vol. 20, 1966, pp. 6–11.

[17]Gatterer, A., *Grating Spectrum of Iron*, Vatican Press, The Vatican, Italy, 1951.

[18]Stair, R., Johnston, R. G., and Halbach, E. W., "Standard of Spectral Radiance for the Region of 0.25 to 2.6 Microns," *Journal of Research of the National Bureau of Standards—A. Physics and Chemistry*, Vol. 64A, 1960, pp. 291–296.

[19]MacPherson, H. G., "The Carbon Arc as a Radiation Standard," *Journal of the Optical Society of America*, Vol. 30, 1940, pp. 189–194.

[20]Null, M. R., and Lozier, W. W., "Carbon Arc as a Radiation Standard," *Journal of the Optical Society of America*, Vol. 52, 1962, pp. 1156–1162.

[21]Flemming, J. C., "An Evaluation of a High Temperature Blackbody as a Working Standard of Spectral Radiance," *Applied Optics*, Vol. 5, 1966, pp. 195–200.

[22]Bowen, S. W., "Spectroscopic and Optical Studies of a High Pressure, Underexpanded Jet," AIAA Paper 66-164, New York, 1966.

[23]Adock, B. D., "Temperature Measurements on a Subatmospheric Argon Plasma Jet," *Journal of Quantitative Spectroscopy & Radiative Transfer*, Vol. 7, 1967, pp. 385–400.

[24]Greenshields, D. H., "Spectrometric Measurements of Gas Temperatures in Arc-Heated Jets and Tunnels," NASA TN D-1960, 1963.

[25]Park, C., "Comparison of Electron and Electronic Temperatures in Recombining Nozzle Flow of Ionized Nitrogen-Hydrogen Mixture. Part 2. Experiment," *Journal of Plasma Physics*, Vol. 9, Pt. 2, 1973, pp. 217–234.

[26]Green, L. C., Johnson, N. C., and Kolchin, E. K., "Oscillator Strengths for Singlet and Triplet Series of Neutral Helium," *Astrophysical Journal*, Vol. 144, 1966, pp. 369–375.

[27]Martin, W. C., "Energy Levels and Spectrum of Neutral Helium (^{4}He I)," *Journal of Research of the National Bureau of Standards, Section A (Phys-Chem)*, Vol. 64, 1960, pp. 19–28.

[28]Herzberg, G., *Molecular Spectra and Molecular Structure, I. Spectra of Diatomic Molecules, 2nd Ed.*, D. Van Nostrand Co., Princeton, NJ, 1950.

[29]Whiting, E. E., Arnold, J. O., and Lyle, G. C., "A Computer Program for a Line-by-Line Calculation of Spectra from Diatomic Molecules and Atoms Assuming a Voight Profile," NASA TN D-5088, 1964.

[30]Blackwell, H. E., Yuen, E., Arepalli, S., and Scott, C. D., "Nonequilibrium Shock Layer Temperature Profiles from Arc Jet Radiation Measurements," AIAA Paper 89-1679, 1989.

[31]Park, C., "Nonequilibrium Air Radiation (NEQAIR) Program: Users Manual," NASA TM-86707.

[32]Park, C., "Calculation of Nonequilibrium Radiation in the Flight Regimes of Aeroassisted Orbital Transfer Vehicles," *Thermal Design of Aeroassisted Orbital Transfer Vehicles*, edited by H. F. Nelson, Vol. 96, Progress in Astronautics and Aeronautics, 1985, pp. 395–418.

[33]Miner, E. W., and Lewis, C. H., "Hypersonic Ionizing Air Viscous Shock-Layer Flows over Nonanalytical Blunt Bodies," NASA CR-2550, May 1975.

[34]Blackwell, H. E., Wierum, F. A., and Scott, C. D., "Spectral Determination of Nitrogen Vibrational Temperatures," AIAA Paper 87-1532, 1987.

[35]Blackwell, H. E., Arepalli, S., Yuen, E., and Scott, C. D., "Analysis of N_2 Shock Layer Emission and the Measurement of Arc Jet Temperatures," AIAA Paper 90-1736, 1990.

[36]Fishburne, E. S., and Petrie, S. L., "Spectrographic Analysis of Plasma Flows," Ohio State Univ. Research Foundation, Rept. ASD-TDR-63-98, Contract AF 33(657)-7561, Columbus, OH, 1963.

[37]Valentin, P., Terrier, M., Vervisch, P., and Piar, G., "Laminar Boundary Layers in Low Pressure Argon Plasma," *Dynamics of Ionized Gases*, edited by M. J. Lighthill, I. Imai, and H. Sato, Wiley, New York, 1971.

[38]Arepalli, S., "Demonstration of the Feasibility of Laser-Induced Fluorescence for Arc Jet Flow Diagnostics," NASA CR-185595, 1989.

[39]Boiarski, A. A., and Daum, F. L., "An Application of Laser-Raman-Spectroscopy to Thermochemical Measurements in an Arc-Heated Wind Tunnel Flow," ARL-72-0126, 1973.

[40]Arepalli, S., Yuen, E. H., and Scott, C. D., "Applications of Laser-Induced Fluorescence for Flow Diagnostics in Arc Jets," AIAA Paper 90-1763, 1990.

[41]Petrie, S. L., *Proceedings of the 1965 Heat Transfer and Fluid Mechanics Institute*, Stanford Univ. Press, Stanford, CA, 1965, p. 17.

[42]Sebacher, D. I., *Proceedings of the 1966 Heat Transfer and Fluid*

Mechanics Institute, Stanford Univ. Press, Stanford, CA, 1966, p. 18.

[43]Petrie, S. L., and Lazdinis, S. S., "Direct Analysis of the Properties of Molecular Oxygen in Hypervelocity Flows," AIAA Paper 69-329, 1969.

[44]Lazdinis, S. S., and Carpenter, R. F., "Nitrogen Temperature Determination in Arc Tunnel Air Flows," AIAA Paper 68-1022, 1972.

[45]Petrie, S. L., "Application of an Electron Beam to High Density Flows of N_2, O_2, and NO," Ohio State Univ., Air Force Flight Dynamics Laboratory-TR-147, OH, Dec. 1976.

[46]Cason, C., "On Some Applications and Problems of an Electron Beam Probe for Plasma Arc Wind Tunnels," AIAA Paper 68-469, 1968.

[47]Trochan, A. M., "Measurements of Parameters for Gas Flows by Means of a Beam of Fast Electrons," *Applied Mechanics and Physics 3*, Vol. 81, 1964.

[48]Anderson, A. D., and Griem, H. R., "Continuum Emission Coefficients Form the Quantum Defect Method," *Proceedings of the 6th International Conference on Ionization Phenomena in Gases*, Vol. 3, North Holland, Amsterdam, 1963, pp. 293–295.

[49]Griem, H. R., *Plasma Spectroscopy*, McGraw-Hill, New York, 1964.

[50]Brown, T. S., and Rose, D. J., "Plasma Diagnostics Using Lasers: Relations Between Scattered Spectrum and Electron-Velocity Distribution," *Journal of Applied Physics*, Vol. 37, 1966, pp. 2709–2714.

[51]Michels, C. J., Rose, J. R., and Sigman, D. R., "Temporal Survey of Electron Number Density and Electron Temperature in the Exhaust of a Megawatt MPD—Arc Thruster," AIAA Paper 72-209, Jan. 1972.

[52]Duckett, R. J., and Jones, W. L., Jr., "Free-Stream Electron Concentration in an Arc Heated Wind Tunnel and Correlation of Langmuir Probe and Microwave Interferometer Measurements," NASA TN D-5500, 1969.

[53]Kamimoto, G., and Nishida, M., "Langmuir Probe Measurements in an Argon Plasma Flow," Dept. of Aeronautical Engineering Kyoto Univ., CP 8, Kyoto, Japan, Nov. 1965.

[54]Poissant, G., and Dudeck, M., "Velocity Profiles in a Rarefied Argon Plasma Stream by Crossed Electrostatic Probes," *Journal of Applied Physics*, Vol. 58, 1985, pp. 1772–1779.

[55]Founoune, M., Danton, C., and Dudeck, M., "Stationary Free Jets of Nitrogen Plasma," *Proceedings of the 15th International Symposium on Rarefied Gas Dynamics*, Grado, Italy, 1988.

[56]Lasgorceix, P., Dudeck, M., and Caressa, J., "Measurements in Low Pressure, High Temperature and Reactive Nitrogen Jets," AIAA Paper 89-1919, June 1989.

[57]Park, C., "Comparison of Electron and Electronic Temperatures in Recombining Nozzle Flow of Ionized Nitrogen-Hydrogen Mixture. Part 1—Theory," *Journal of Plasma Physics*, Vol. 9, Pt. 2, 1973, pp. 187–215.

[58]Beth, M.-U., and Kling, M. G., "Spectroscopically Measured Velocity Profiles of an MPD Arcjet," *AIAA Journal*, Vol. 7, No. 11, 1969, pp. 2181, 2182.